geodiversitas

2026 • 48 • 7

Bone microanatomy and weight-bearing adaptations in the giant proboscidean *Deinotherium giganteum* (Kaup, 1829)

Camille BADER,
Mihály GASPARIK
& Martin SEGESDI

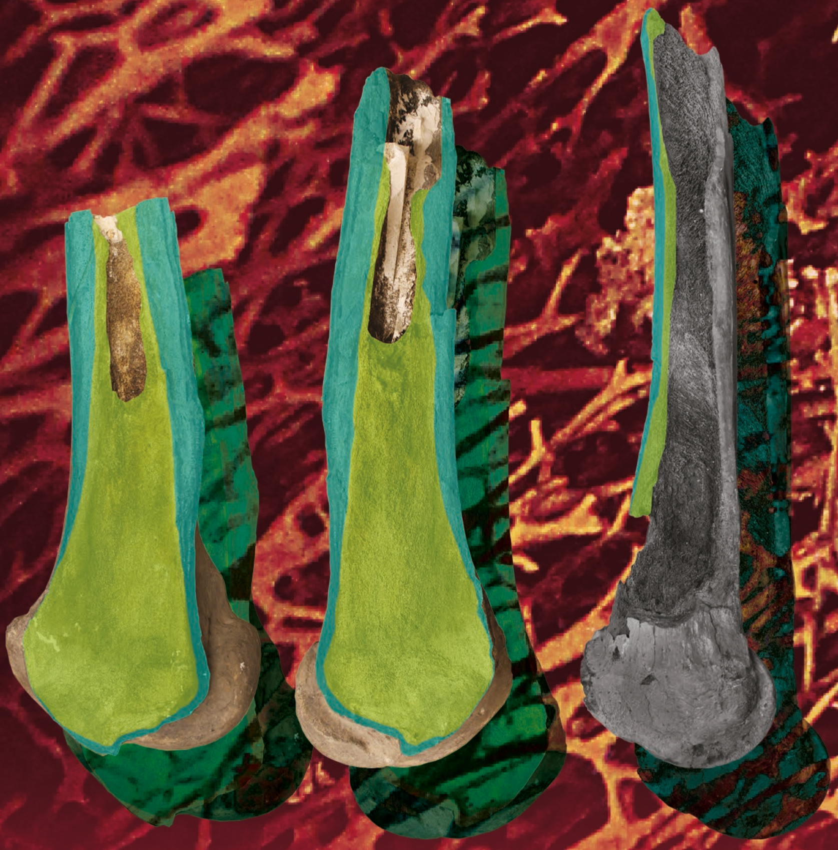

art. 48 (7) — Published on 16 April 2026
www.geodiversitas.com

PUBLICATIONS
SCIENTIFIQUES

Directeur de la publication / *Publication director* : Gilles Bloch,
Président du Muséum national d'Histoire naturelle

Rédacteur en chef / *Editor-in-chief* : Sylvain Charbonnier

Rédacteur associé / *Associate editor*: Didier Merle

Éditeur technique (suivi éditorial) / *Desk editor (editorial process)* : Emmanuel Côtez (geodiv@mnhn.fr)

Éditeur technique (production) / *Desk editor (production)* : Emmanuel Côtez

Comité scientifique / *Scientific board* :
Christine Argot (Muséum national d'Histoire naturelle, Paris)
Beatrix Azanza (Museo Nacional de Ciencias Naturales, Madrid)
Raymond L. Bernor (Howard University, Washington DC)
Henning Blom (Uppsala University)
Gaël Clément (Muséum national d'Histoire naturelle, Paris)
Ted Daeschler (Academy of Natural Sciences, Philadelphie)
Cédric Del Rio (Muséum national d'Histoire naturelle)
Gregory D. Edgecombe (The Natural History Museum, Londres)
Ursula Göhlich (Natural History Museum Vienna)
Jin Meng (American Museum of Natural History, New York)
Brigitte Meyer-Berthaud (CIRAD, Montpellier)
Zhu Min (Chinese Academy of Sciences, Pékin)
Isabelle Rouget (Muséum national d'Histoire naturelle, Paris)
Sevket Sen (Muséum national d'Histoire naturelle, Paris, retraité)
Stanislav Štamberg (Museum of Eastern Bohemia, Hradec Králové)
Paul Taylor (The Natural History Museum, Londres, retraité)

Couverture / *Cover* :
Réalisée à partir des Figures de l'article/*Made from the Figures of the article*.

Geodiversitas est indexé dans / Geodiversitas *is indexed in:*
- Science Citation Index Expanded (SciSearch®)
- ISI Alerting Services®
- Current Contents® / Physical, Chemical, and Earth Sciences®
- Scopus®

Geodiversitas est distribué en version électronique par / Geodiversitas *is distributed electronically by:*
- BioOne® (http://www.bioone.org)

Les articles ainsi que les nouveautés nomenclaturales publiés dans *Geodiversitas* sont référencés par /
Articles and nomenclatural novelties published in Geodiversitas *are referenced by:*
- ZooBank® (http://zoobank.org)

Geodiversitas est une revue en flux continu publiée par les Publications scientifiques du Muséum, Paris
Geodiversitas *is a fast track journal published by the Museum Science Press, Paris*

Les Publications scientifiques du Muséum publient aussi / *The Museum Science Press also publish:* ***Adansonia***, ***Zoosystema***, ***Anthropozoologica***,
European Journal of Taxonomy, ***Naturae***, ***Cryptogamie*** **sous-sections** ***Algologie***, ***Bryologie***, ***Mycologie***, ***Comptes Rendus Palevol***

Diffusion – Publications scientifiques Muséum national d'Histoire naturelle
CP 41 – 57 rue Cuvier F-75231 Paris cedex 05 (France)
Tél. : 33 (0)1 40 79 48 05 / Fax : 33 (0)1 40 79 38 40
diff.pub@mnhn.fr / http://sciencepress.mnhn.fr

Les articles publiés dans *Geodiversitas* sont distribués sous licence CC-BY 4.0/*Articles published in* Geodiversitas *are distributed under a CC-BY 4.0 license*.
ISSN (imprimé / *print*) : 1280-9659/ ISSN (électronique / *electronic*) : 1638-9395

Bone microanatomy and weight-bearing adaptations in the giant proboscidean *Deinotherium giganteum* (Kaup, 1829)

Camille BADER
Muséum national d'Histoire naturelle, Département Adaptations du Vivant, UMR 7179,
Mécanismes adaptatifs et Évolution (MECADEV), MNHN, CNRS,
case postale 38, 57 rue Cuvier, F-75231 Paris cedex 05 (France)
camille.bader@edu.mnhn.fr (corresponding author)

Mihály GASPARIK
Hungarian National Museum Public Collection Centre, Budapest,
Hungarian Natural History Museum, Department of Paleontology and Geology,
H-1083 Budapest, Ludovika tér 2. (Hungary)
gasparik.mihaly@nhmus.hu

Martin SEGESDI
Hungarian National Museum Public Collection Centre, Budapest,
Hungarian Natural History Museum, Department of Zoology,
Department of Paleontology and Geology, H-1083 Budapest, Ludovika tér 2. (Hungary)
and ELTE Eötvös Loránd University, Institute of Geography and Earth Sciences,
Department of Paleontology, H-1117 Budapest, Pázmány Péter sétány 1/c (Hungary)
martinsegesdi@gmail.com

Submitted on 14 April 2025 | accepted on 10 June 2025 | published on 16 April 2026

urn:lsid:zoobank.org:pub:F30CD99A-E3AA-4E38-A915-8411FC2A0061

Bader C., Gasparik M. & Segesdi M. 2026. — Bone microanatomy and weight-bearing adaptations in the giant proboscidean *Deinotherium giganteum* (Kaup, 1829). *Geodiversitas* 48 (7): 127-143. https://doi.org/10.5252/geodiversitas2026v48a7. http://geodiversitas.com/48/7

ABSTRACT

Bone anatomy reflects the mechanical and functional constraints to which the skeleton is subjected. In graviportal taxa, the primary constraint is gravity, requiring specific adaptations in bone structure. Proboscideans, including modern elephants and their fossil relatives, illustrate these adaptations, notably through a columnar posture that optimizes load transmission. While adaptations of external bone morphology have been described within this order, variations in bone microanatomy have rarely been studied in fossil proboscideans. In this study, we analyze for the first time the microanatomy of a *Deinotherium giganteum* (Kaup, 1829) femur, a fossil species from the Deinotheriidae Bonaparte, 1845 family, based on a fractured specimen preserved at the Hungarian Natural History Museum. We compare these observations with those of a *Mammuthus* sp. femur to assess similarities and differences in weight-bearing adaptations across different proboscidean families. Our results reveal shared characteristics between the two taxa, including a thick-walled diaphysis, a medullary cavity largely filled with trabecular tissue, and highly anisotropic trabeculae aligned with axial loading, features also observed in modern elephants. However, *D. giganteum* exhibits a more pronounced hourglass-shaped cortical distribution and relatively greater cortical thickness than *Mammuthus* sp., suggesting differences in load distribution or distinct weight-bearing adaptation strategies between these two taxa.

KEY WORDS
Proboscidea,
Deinotherium,
functional morphology,
femur,
bone microanatomy.

RÉSUMÉ
Microanatomie osseuse et adaptation au support de la masse chez le proboscidien géant Deinotherium giganteum *(Kaup, 1829).*
L'anatomie osseuse reflète les contraintes mécaniques et fonctionnelles auxquelles le squelette est soumis. Chez les taxons graviporteurs, la contrainte principale est la gravité, nécessitant des adaptations particulières de la structure osseuse. Les proboscidiens, comprenant les éléphants actuels et leurs parents fossiles, illustrent ces adaptations, notamment à travers une posture colonnaire qui optimise la transmission de la charge mécanique. Bien que les adaptations de la morphologie externe des os aient été décrites au sein de cet ordre, les variations de la microanatomie osseuse n'ont été que rarement étudiées chez les proboscidiens fossiles. Dans cette étude, nous analysons pour la première fois la microanatomie du fémur de *Deinotherium giganteum* (Kaup, 1829), une espèce fossile de la famille des Deinotheriidae Bonaparte, 1845, à partir d'un spécimen fracturé conservé au Musée national Hongrois d'Histoire naturelle. Nous comparons ces observations avec celles d'un fémur de *Mammuthus* sp. afin d'évaluer les similarités et différences dans l'adaptation au support d'un poids massif au sein de différentes familles de proboscidiens. Nos résultats révèlent des caractéristiques communes aux deux taxons, incluant une diaphyse à paroi épaisse, une cavité médullaire largement remplie de tissu trabéculaire et des trabécules hautement anisotropes alignées avec la charge axiale, des traits également observés chez les éléphants actuels. Cependant, *D. giganteum* présente une distribution corticale plus marquée en forme de sablier et une épaisseur corticale relative plus importante que *Mammuthus* sp., suggérant des différences dans la répartition des charges ou différentes stratégies d'adaptations au support du poids entre ces deux taxons.

MOTS CLÉS
Proboscidea,
Deinotherium,
morphologie fonctionnelle,
fémur,
microanatomie osseuse.

INTRODUCTION

The vertebrate skeleton provides a rigid structure that supports and enables movement of the body. Like all biological structures, limb anatomy results from the conjoined effects of phylogenetic, structural and functional constraints (e.g., Gould 2002; Cubo 2004). Bone microanatomy (i.e., the organization of the bony tissues) provides crucial information on the constraints the animals are facing. The internal structure of bones, including their density, cortical thickness, and arrangement of bone tissues, allow for inferences regarding the stresses that are placed on the bones. When subjected to mechanical loading, bones undergo structural adaptations to better support the increased stress placed upon them (Ruff & Hayes 1983; Turner 1998; Ruimerman 2005; Habib & Ruff 2008; Nikander *et al.* 2010; Doube *et al.* 2011; Bishop *et al.* 2018). In the case of giant terrestrial animals, the greatest challenge of the skeleton is resistance to gravity: gravity exerts a downward force proportional to an animal's body mass (Biewener 1989; Bertram & Biewener 1990; Biewener & Patek 2018). As body length doubles isometrically, body mass increases by a factor of 8 (Schmidt-Nielsen 1984), meaning that larger animals contend with relatively greater gravitational constraints compared to smaller ones. Giant quadrupeds are thus particularly challenged: some of them exhibit distinctive musculoskeletal and physiological adaptations allowing them to accommodate their massive weight, and are generally termed as graviportal (e.g. elephants, rhinoceroses, hippopotamuses, sauropodomorph dinosaurs). This term was originally proposed by Gregory (1912) and Osborn (1929), and refers to an ensemble of morphological and locomotor traits that facilitate weight-bearing. These traits include columnar limbs, relatively lengthened stylopods and shortened autopods, robust long bones (i.e., wider diaphyses for a given length), and enlarged feet with thick adipose cushions (Gregory 1912; Osborn 1929; Hildebrand 1974; Coombs 1978; Alexander & Pond 1992; Langman *et al.* 1995; Hutchinson *et al.* 2003). These features are typically associated with a high body mass (over several hundred kilograms) and limited locomotor capabilities, such as an inability to gallop. However, the concept of graviportality remains debated (Coombs 1978; Carrano 1999; Mallet *et al.* 2019). While extant elephants are the perfect example of graviportality, fulfilling all anatomical and functional criteria, other heavy terrestrial mammals (e.g., rhinoceroses and hippos) only partially conform to the definition. Rhinoceroses, although massive and morphologically adapted to weight-bearing, retain the ability to gallop, leading early authors to consider them mediportal (Gregory 1912; Osborn 1936), although they have since been reclassified as graviportal by others (Prothero & Sereno 1982; Eisenmann & Guérin 1984). Similarly, hippos have been variably categorized due to their capacity to trot and their semi-aquatic adaptations (Ross 1984; Alexander & Pond 1992; Carrano 1999; Stilson *et al.* 2016; Hutchinson & Pringle 2024). Beyond external morphology, graviportal animals also show microanatomical specializations in the limb bones (Gregory 1912; Osborn 1936; Coombs 1978; Mallet *et al.* 2019, 2020; Lefebvre *et al.* 2022; Bader *et al.* 2025, in press). These include the reduction or absence of a medullary cavity and increased compactness of bone tissue, which improve resistance to high compressive forces and enhance load distribution (Wall 1983; Houssaye *et al.*

2016, 2018; Nganvongpanit *et al.* 2017; Lefebvre *et al.* 2023; Bader *et al.* in press). Increased bone density and thickened cortices also improve resistance to bending and torsional loads (Currey & Alexander 1985; Oxnard 1990, 1993; Houssaye *et al.* 2016; Canoville *et al.* 2022): extant elephant display a distinctive cortical bone distribution, forming an "hourglass" or dual-cone pattern centered around the growth center (GC). In the absence of secondary bone deposition in the medullary cavity, this thickening occurs primarily where compact bone is initially laid down. The thicker cortex enhances resistance to compressive loads and likely corresponds to zones of peak stress during loading, helping maintain mechanical safety. Similar patterns have been described in extant rhinoceroses (Etienne 2023) and hippos (Houssaye *et al.* 2021), where reduced bone resorption near the GC preserves cortical thickness under high stresses, as indicated by trabecular anisotropy (i.e. trabeculae oriented preferentially along an axis). While some large sauropods also show cortical thickening near the GC, it is less pronounced, implying alternative weight-bearing adaptations (Lefebvre *et al.* 2023). Finally, the limb long bones of graviportal taxa show highly anisotropic trabeculae, oriented orthogonally to the ground (Wall 1983, Lefebvre *et al.* 2023; Etienne 2023) in columnar taxa such as sauropod dinosaurs and graviportal proboscideans, the trabeculae are thus oriented in a mostly parallel manner to the long axis of the limb bones, maximizing the axial distribution of the load (Lefebvre *et al.* 2023, Bader *et al.* 2025).

The order Proboscidea Illiger, 1811 includes some of the largest terrestrial animals to have ever lived (Sukumar 1992; Larramendi 2016). Some species reached gigantic sizes, exceeding 5 meters at the shoulder and weighing up to 22 tons (Meshram & Sonakia 2006; Larramendi 2016). Today, the group is represented by only three species of elephants (Wilson *et al.* 2011), which remain the heaviest living land mammals. However, early proboscideans were far smaller (Sukumar 1992; Shoshani & Tassy 2005). The order comprises over 180 extinct species (Kingdon & Happold 2013) that once inhabited every continent except Oceania and Antarctica (Cantalapiedra *et al.* 2021). The earliest forms, such as *Eritherium* Gheerbrant, 2009 and *Phosphatherium* Gheerbrant, Sudre & Cappetta, 1996, from the Paleocene of Northern Africa, weighed only 6 to 17 kg (Gheerbrant *et al.* 2005; Gheerbrant & Tassy 2009; Larramendi 2016). Larger taxa emerged during the Eocene and Oligocene (e.g., *Barytherium* Andrews, 1901, *Palaeomastodon* Andrews, 1901, *Chilgatherium* Sanders, Kappelman & Rasmussen, 2004) weighing over 1500 kg (Larramendi 2016). From the Miocene onward, proboscideans underwent a marked size increase across all families (Tassy 1990; Cantalapiedra *et al.* 2021), with many species exceeding 10 tons (e.g. *Deinotherium giganteum* (Kaup, 1829), *Mammuthus trogontherii* (Pohlig, 1885)) and some approaching 20 tons, including *Palaeoloxodon antiquus* (Falconer & Cautley, 1847) and "*Mammut*" *borsoni* (Hays, 1834). Extant elephants (like other graviportal taxa) exhibit distinct microanatomical adaptations in their limb long bones to support their massive body weight (Wall 1983; Houssaye *et al.* 2016; Nganvongpanit *et al.* 2017; Etienne 2023; Lefebvre *et al.* 2023; Bader *et al.* 2024). In proboscideans, gigantism was facilitated in part by the acquisition of the columnar stance, where the limbs are straight and nearly perpendicular to the ground at rest. This alignment allows an increased reliance on axial compression, enabling the support of several tons of body mass without a proportional increase in bone robustness (Hildebrand 1974). As a result of the limb orientation, extant elephants have been shown to exhibit highly anisotropic trabeculae, primarily oriented orthogonally to the ground, optimizing load transmission along the columnar limbs (Bader *et al.* 2025). While the microanatomical adaptations of limb bones have been documented in modern elephants (Nganvongpanit *et al.* 2017; Bader *et al.* 2025) and, to some extent, in several extinct dwarf elephantids (Köhler *et al.* 2021; Bader *et al.* in press), they remain largely unstudied across the rest of the proboscidean order. In particular, the microanatomical variations associated with the acquisition of a columnar posture are still poorly understood. Among proboscideans, the Deinotheriidae Bonaparte, 1845 family was the first to display columnar limbs, and while the morphological variation of their long bones has been described (Bader *et al.* 2024), their microanatomy has yet to be explored.

The scarcity of proboscidean fossil material often limits their inclusion in studies requiring destructive analysis. Furthermore, practical constraints, such as the sheer size of the bones, often prevent the use of micro-CT scanning as a non-invasive method for examining their microstructure. While the bones might fit in conventional medical CT, the resolution of such devices is not high enough to provide detailed visualizations of the microanatomy. The Hungarian Natural History Museum (HNHM) collection in Budapest (Hungary) contains a unique *Deinotherium giganteum* (Kaup, 1829) femur that was previously split in two. This resulted in a longitudinally segmented bone with minimal alteration to its internal structure, providing rare and valuable insights into the microanatomy of the giant Deinotheriidae. The Deinotheriidae originated in the Oligocene of Northern Africa, and later spread across Europe and Asia during the Miocene. This family includes three genera (*Chilgatherium, Prodeinotherium* Éhik, 1930, *Deinotherium*) with species ranging from 4 to 12 tons, and is the first proboscidean family to display a columnar stance. This postural adaptation is considered as a synapomorphy of these two apical clades (deinotheres and elephantiforms), although deinotheres display distinct morphological variations in their limb bones as compared to more derived proboscideans. Notable differences, such as a larger greater tubercle of the humerus and a reduced anconeal process of the ulna, suggest potential differences in posture and weight distribution (Bader *et al.* 2024). These variations raise the question of whether Deinotheriidae share the same microanatomical adaptations for heavy weight-bearing as modern proboscideans and whether the acquisition of a columnar posture is reflected similarly across phylogenetically distant proboscidean taxa. The specimen studied here will thus provide a

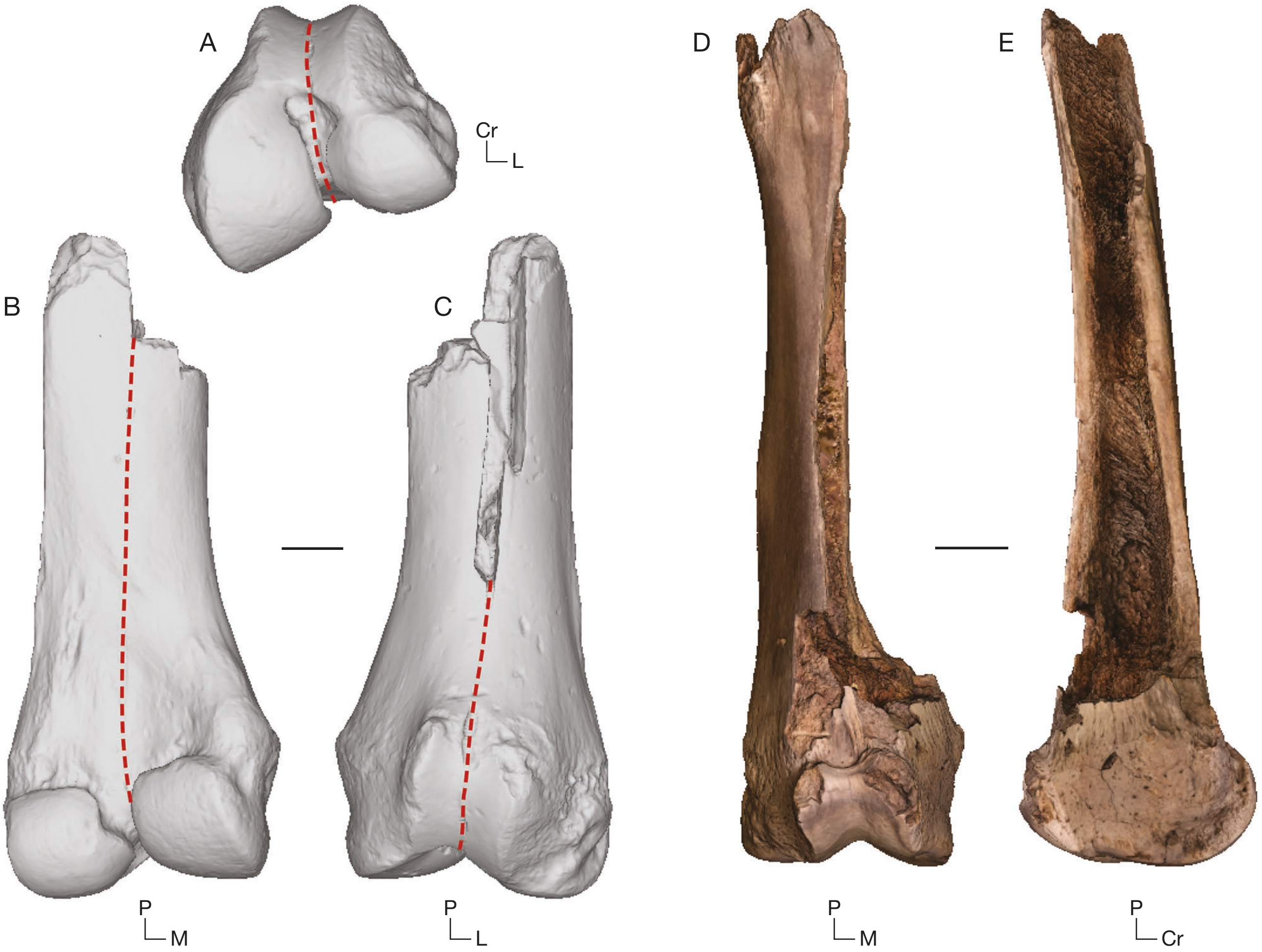

FIG. 1. — 3D model reconstruction of the *Deinotherium giganteum* (Kaup, 1829) femur (HNHM-V.79.166.) in distal (**A**), caudal (**B**) and cranial (**C**) views and of the *Mammuthus* sp. femur (HNHM-PAL 2025.5.1.) in cranial (**D**) and medial (**E**) views. **Dotted line** indicates the boundary between the two reconstructed fragments of HNHM-V.79.166. Abbreviations: **Cr**, cranial; **M**, medial; **L**, lateral; **P**, proximal. 3D models by Camille Bader. Scale bars: 10 cm.

unique opportunity to further our understanding of limb anatomy evolution in proboscideans in relation to body mass. In addition to the *Deinotherium* femur, the collection includes another damaged proboscidean femur (probably from the genus *Mammuthus* Brookes, 1828), providing another rare opportunity to observe the inner bone structure of a fossil proboscidean species. Since *Mammuthus* is more closely related to extant elephants than *Deinotherium*, we expect its microstructure to show greater similarity to other elephantids. This comparison will allow us to assess whether phylogenetically closer species exhibit greater microanatomical resemblance or if weight-bearing demands override phylogeny, leading to similar structural adaptations in both deinotheres and elephantids.

In this study, we aim to: 1) provide the first description of the microanatomy of a *Deinotherium giganteum* femur, taking trabecular density and orientation as well as variations in cortical thickness into account; 2) compare our observations to the microanatomy of a *Mammuthus* sp. femur; and 3) contextualize these findings within the broader framework of weight-bearing adaptations in proboscideans (limb posture, bone external morphology).

MATERIAL AND METHODS

SAMPLE

Our sample is composed of two partial bones from the Palaeovertebrate Collection of the Hungarian Natural History Museum (HNHM) in Budapest, Hungary. Due to historical reasons, very little written information is now available regarding these specimens, so that only one of the two specimens could be identified at the species level.

Deinotherium giganteum *femur*

The specimen was provisionally assigned the ID “Deinotheriumsp001” in a previous study (Bader *et al.* 2024) due to uncertainty regarding its original catalog number. However, curatorial work since then has revealed that it is part of the material inventoried as *Deinotherium giganteum* (body mass: *c.* 12 000 kg; Larramendi 2016) under the number HNHM-V.79.166.

The HNHM-V.79.166. specimen (femur + tibia) today consists of six fragments. The femur is in four pieces, including the distal half of the bone split in two (Fig. 1A, B, C), a smaller proximal diaphyseal fragment, and a part of the

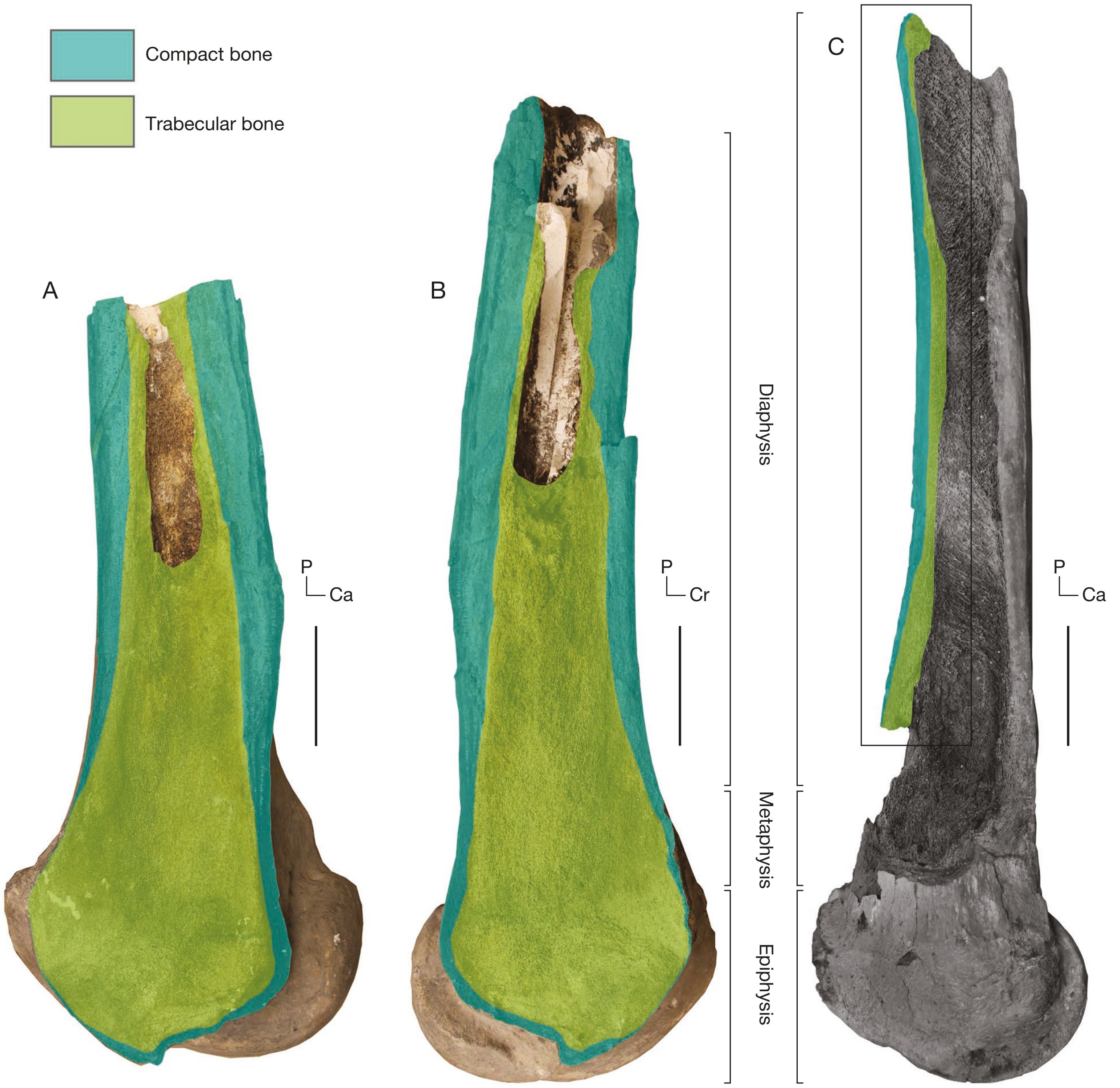

Deinotherium giganteum (Kaup, 1829)

Mammuthus sp.

Fig. 2. — Distribution of the bony tissues in the femur of: **A**, **B**, *Deinotherium giganteum* (Kaup, 1829) (specimen HNHM-V.79.166); **B**, lateral view; **C**, *Mammuthus* sp. (specimen HNHM-PAL2025.5.1), medial view. Abbreviations: **Ca**, caudal; **Cr**, cranial; **P**, proximal. Photos by Camille Bader and Martin Segesdi. Scale bars: 10 cm.

greater trochanter (Fig. 6[S1]). The tibia consists of the proximal epiphysis in two parts (Fig. 7[S2]). The distal half of the femur had been previously digitized via photogrammetry for a study on proboscidean limb bones (Bader *et al.* 2024), and 3D models of the two segments were digitally reassembled to reconstruct the femur, providing a visualization of its distal morphology. The bone was split along its longitudinal axis (Fig. 1A-C), with minimal additional alteration, allowing for a rare longitudinal view of the internal architecture of a *D. giganteum* femur, extending from the intercondylar fossa to approximately the mid-diaphysis. The reconstructed distal part of the femur measures 88.43 cm in length. Based on a picture of the complete bone (i.e. before fragmentation), we estimate the original total length of the femur to exceed 150 cm (Fig. 8[S3]), which is well above the known adult range reported in Bader *et al.* (2024). We thus conclude that this femur belonged to an adult individual.

Limited information is available regarding the origin of the *D. giganteum* bones in question. The label indicates that the remains originate from a site belonging to the Pannonian Stage, a regional chronostratigraphic unit which, according to current definitions spans from 11.6 to 2.6 Ma, corresponding to the Late Miocene and Pliocene (Magyar *et al.* 2025). The place of origin is indicated by both the historical Hungarian and the Romanian names of the settlement: “Nántű / Hurezu Mare / Szilágy County”. Today, Hurezu Mare vil-

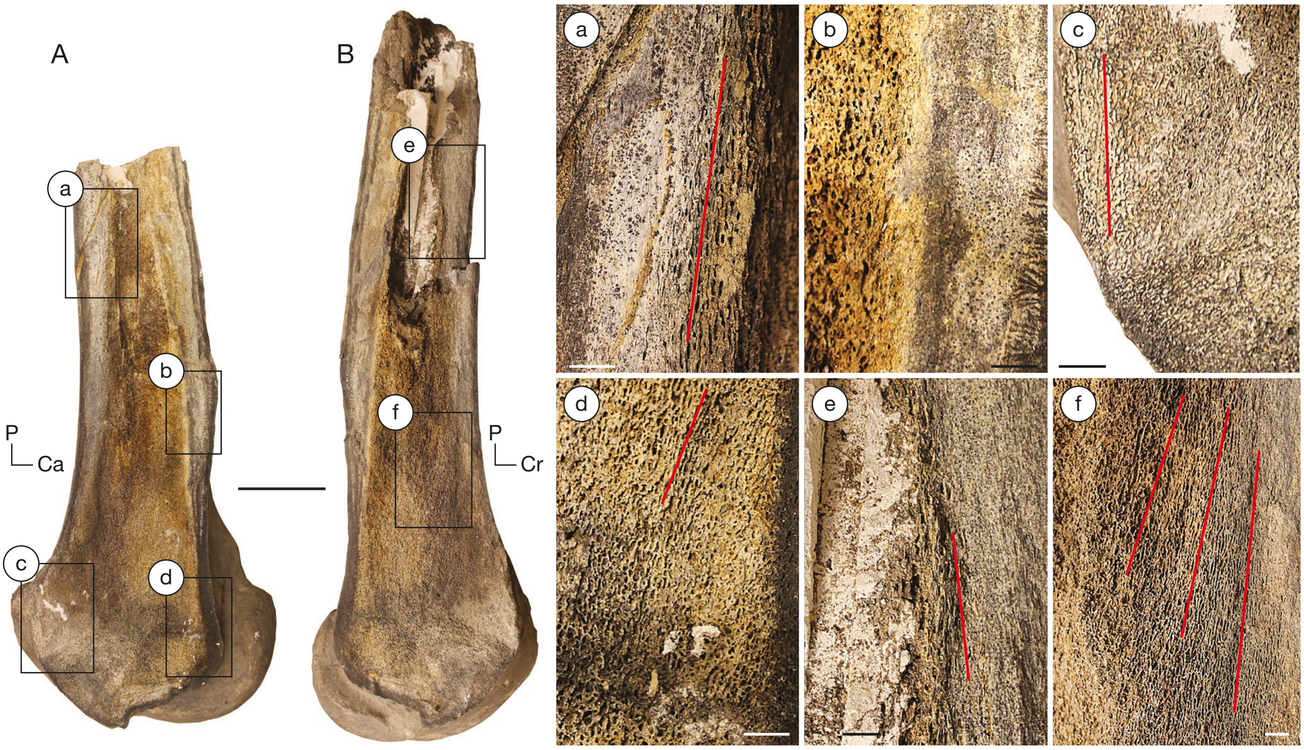

FIG. 3. — General and zoomed-in views of trabecular orientation in the femur of HNHM-V.79.166. of *Deinotherium giganteum* (Kaup, 1829) in medial (**A**) and lateral (**B**) views. Abbreviations: **Ca**, caudal; **Cr**, cranial; **P**, proximal. The **red lines** indicate the direction of the trabeculae in highly anisotropic areas. Photos by Camille Bader and Martin Segesdi. Scale bars: A, B, 10 cm; a-f, 1 cm.

lage is located in Supur Commune in Satu Mare County, northwestern Romania. As the county (and state) borders have changed several times over the last century, so has the county to which Hurezu Mare belonged (Hajdú-Moharos 1997; Szilágyi 2008). The designation “Szilágy county” (Sălaj County in Romanian) might thus offer a clue regarding the collection period, but without further evidence this remains speculative.

Unfortunately, no record has yet been found on the exact location of the site or the identity of the collectors. It is possible that such information was lost or forgotten during the turbulent years of the Second World War, or perhaps during the Hungarian Revolution of 1956. Several *D. giganteum* finds of this age have been recovered from the deposits around Hurezu Mare (for example in neighboring villages such as Supuru de Sus and Derșida) (Apostol 1968; Jurcsák 1973, 1983; Codrea & Andreica 1988; Codrea *et al.* 2002; Codrea 2008). However, our paper is the first to report the closer area of Hurezu Mare as a potential locality for *D. giganteum* bones.

The femur and tibia were part of the former exhibition titled “A Föld és az élet fejlődéstörténete” (“The History of Earth’s and Life’s Evolution”). The bones were supplemented with a replica fibula and distal limb elements, assembled and labeled in the exhibition as “left hind limb of a mastodon” (Fig. 8[S3]). Based on photographs and exhibition guides, the bones must have been in the exhibition hall already in 1954 (Természettudományi Múzeum-Magyar Nemzeti Múzeum 1954; Koroknai 1954). During the Hungarian Revolution of 1956, the museum building was hit by artillery and suffered extensive damage, but the resulting fire fortunately did not affect this particular exhibition area (Boros 1957; Papp 2016). Later, the *Deinotherium* bones appear intact in a newsreel clip from 1961.05.01 (Fig. 9[S4]). No further information is available regarding the later history of the bones or the circumstances of their damage and fragmentation.

Mammuthus *sp. femur*

The specimen HNHM-PAL 2025.5.1. is a femur of an undetermined proboscidean species. This bone was previously digitized using photogrammetry for another study (Bader *et al.* 2024), producing a 3D reference model. Damage to the proximal region of the femoral trochlea prevents the use of geometric morphometric methods (GMMs) to compare it quantitatively with other proboscidean species. However, qualitative comparisons of the distal condyles with those of similarly sized proboscideans (e.g. *Deinotherium*, *Mammut*, *Gomphotherium* Burmeister, 1837, *Mammuthus*) suggest an affinity with *Mammuthus*. Additionally, this specimen is stored among several limb bones of *Mammuthus primigenius* Blumenbach, 1799 (body mass: *c.* 6000 kg; Larramendi 2016), which further supports its identification as *Mammuthus*. Although the HNHM does not currently house limb bone remains of other *Mammuthus* species, the absence of a label or associated documentation prevents a definitive species-level assignment.

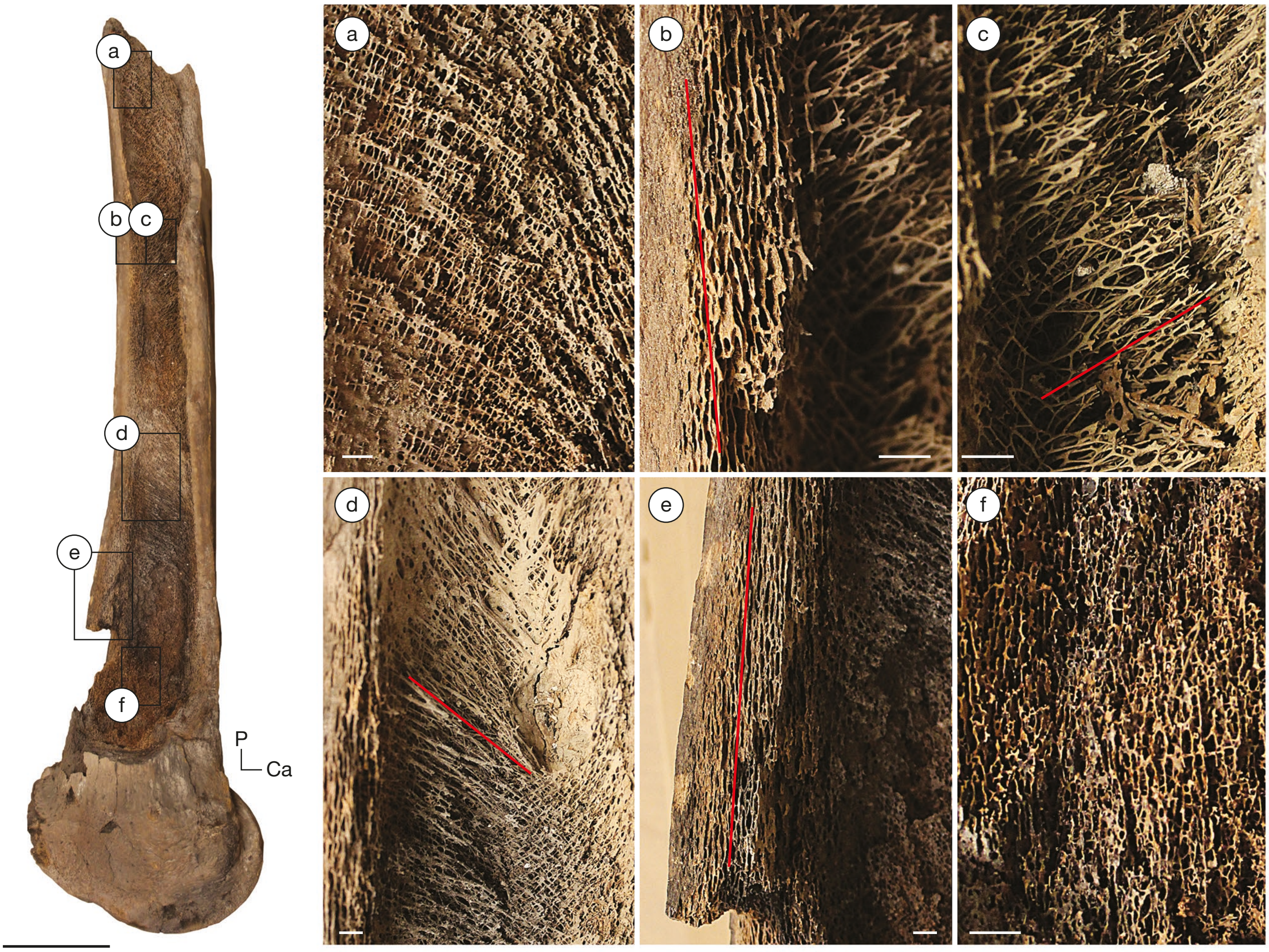

FIG. 4. — General and zoomed-in views of trabecular orientation in the femur of HNHM-PAL 2025.5.1 of *Mammuthus* sp. in medial view. Abbreviations: **Ca**, caudal; **P**, proximal. The **red lines** indicate the direction of the trabeculae in highly anisotropic areas. Photos by Camille Bader and Martin Segesdi. Scale bars: A, B, 10 cm; a-f, 1 cm.

The HNHM-PAL 2025.5.1. specimen consists of a partial femur, lacking the proximal epiphysis and the medial portion of the diaphysis. This preservation state provides an exposed view of the internal bone structure from the distal metaphysis to the proximal metaphysis (Fig. 1D, E). The femur (lacking the proximal epiphysis) measures 114.26 cm in length, which falls well within the adult size range for mammoth femora, regardless of species (Bader *et al.* 2024). We thus conclude that this femur belonged to an adult individual.

IMAGING

Digital photographs of the bones were taken using a Canon EOS 600D camera. Camera settings, including focal length, exposure, and lighting conditions, were standardized across all images to ensure consistency. Pictures were modified in Adobe Illustrator CC (23.0) to highlight the different tissues in the bones, considering the parts that were on a similar level (i.e. not broken at different depths), hence the *Mammuthus* femur being only highlighted in the cranial part of the diaphysis. Zoomed-in images were processed using the 'Unsharp Mask' filter in ImageJ (version 1.52p) to enhance sharpness (radius: 5 px, mask weight: 0.60).

LINEAR MEASUREMENTS

To highlight the differences between the two taxa and provide a quantitative reference for future studies, we measured the absolute maximal thickness of the diaphyseal cortex (*AmaxT*) and the corresponding diaphyseal diameter at that point (*D*). Using these values, we calculated the relative maximal thickness of the diaphyseal cortex (*RmaxT*), defined as the ratio of *AmaxT* to *D*.

RESULTS

DEINOTHERIUM GIGANTEUM FEMUR

In *D. giganteum*, the compact bone is thickest at the mid-diaphysis, with a greater thickness on the caudal side compared to the cranial side (*RmaxT* = 0.36, see Table 1). This compact layer tapers toward the metaphysis and epiphysis (Fig. 2A, B). The compact bone is extremely thin on the cranioproximal side of the femoral trochlea, slightly thicker in its distal portion, and thickest within the intercondylar fossa.

The medullary area is occupied by trabecular bone from the distal epiphysis up to just below the mid-diaphysis. The

TABLE 1. — Linear measurements taken on the two femora of *Deinotherium giganteum* (Kaup, 1829) and *Mammuthus* sp. Abbreviations: **AmaxT**, absolute maximal cortical thickness; **D**, corresponding diaphyseal diameter; **RmaxT**, relative maximal cortical thickness defined as the ratio of AmaxT to D.

Species	Specimen ID	AmaxT (cm)	D (cm)	RmaxT
Deinotherium giganteum	HNHM-V.79.166	4.86	13.51	0.36
Mammuthus sp.	HNHM-PAL 2025.5.1	1.08	9.45	0.11

midshaft remains largely devoid of trabecular bone, though some breakage may have occurred. However, the absence of trabecular bone in this region appears to be natural rather than taphonomic.

The trabeculae are thin and numerous, with a higher density in the distal epiphysis compared to the shaft. In the mid-diaphysis, the trabeculae exhibit high anisotropy, oriented proximodistally and running parallel to the compact bone (Fig. 3a, e). In the distal diaphysis, the outermost layer of trabecular bone consists of highly anisotropic but thinner trabeculae, whereas the innermost region contains thicker, sparser, and mostly isotropic trabeculae (Fig. 3b). Just above the distal metaphysis, the trabeculae are thin and highly anisotropic, oriented from the cranial side to the distocaudal side. This orientation aligns orthogonally to the ground when the femur is at rest, reflecting the slight curvature of the bone in a normal standing position (Fig. 3f). The innermost and caudal regions of the distal diaphysis contain predominantly isotropic trabeculae, while the outermost parts exhibit anisotropic trabeculae oriented orthogonally to the compact bone layer (Fig. 3c). In the cranioproximal portion of the trochlea, the trabeculae are anisotropic and aligned parallel to the articular surface, whereas in the distal trochlea, they are oriented orthogonally to the articular surface. Overall, trabecular anisotropy is more pronounced in the cranial part of the distal metaphysis and epiphysis than in the caudal part (Fig. 3c, d).

MAMMUTHUS SP. FEMUR

In *Mammuthus* sp., the visible portion of the femur reveals a thick compact bone layer at mid-diaphysis, which tapers distally toward the distal epiphysis but shows a similar thickness proximally (RmaxT = 0.11, see Table 1), extending toward the greater trochanter (Fig. 2C). The distal epiphysis is filled with trabecular bone, with fractured trabeculae in the distal metaphysis, suggesting that this area was originally also filled with trabecular bone.

A thick layer of trabecular bone, approximately one-quarter of the shaft's diameter, is present along the outermost parts of the diaphysis, while the inner regions remain largely free of trabecular bone. In the proximal metaphysis, distal to the greater trochanter, the trabecular layer is notably thin but thickens again closer to the greater trochanter itself.

In the proximal metaphysis, the trabeculae are thick and arranged in large lattice-like structures, forming arching patterns from the cranioproximal side of the shaft to the distocaudal side (Fig. 4a). In the proximal and mid-diaphysis, the trabeculae remain thick and highly anisotropic, with those in the outermost regions oriented parallel to the compact bone. In the inner regions, many trabeculae appear broken, but the intact ones are oriented from proximocaudal to craniodistal, forming lattices of thick and widely spaced trabeculae (Fig. 4b, c). Just below the mid-diaphysis, distal to the growth center (GC), the trabeculae maintain a similar thickness but oriented in the opposite way, with the inner trabeculae arranged from proximocranial to distocaudal. The trabeculae in the outermost regions remain parallel to the compact bone (Fig. 4d, e). Above the distal metaphysis, the trabecular tissue is largely fragmented. However, the remaining trabeculae are much thinner and show a much lower anisotropy, suggesting that the original metaphysis was filled with isotropic or lowly anisotropic trabeculae oriented proximodistally (Fig. 4e, f). The fractured lateral portion of the trochlea reveals isotropic trabeculae in the inner part of the structure, while the outermost trabeculae are anisotropic and aligned parallel to the compact bone (Fig. 5). On the medial side, the broken region of the trochlea primarily consists of isotropic trabeculae, with a faint orthogonal orientation to the compact layer in the most proximal part (Fig. 5).

DISCUSSION

GENERAL PATTERN AND WEIGHT-BEARING ADAPTATIONS

This study provides preliminary insights into the microanatomy of the femur of *D. giganteum* and *Mammuthus* sp., suggesting that both taxa share similar microanatomical patterns adapted to massive weight-bearing. Both specimens exhibit femora with a relatively thick cortex, a medullary area filled with trabecular bone except in the mid-diaphysis, and highly anisotropic trabeculae oriented orthogonally to the ground. These characteristics are expected in graviportal animals (Houssaye *et al.* 2016; Lefebvre *et al.* 2023), including proboscideans (Bader *et al.* 2025, in press).

The femur of *D. giganteum* exhibits a distinctive cortical bone distribution, characterized by thickening around the growth center, resulting in an hourglass-shaped pattern. While this feature is less prominent in *Mammuthus*, it remains discernible. Similar distributions have been observed in modern elephants (Nganvongpanit *et al.* 2017; Bader *et al.* 2025) and other large-bodied taxa, including extant rhinoceroses (Etienne, 2023) and hippopotamuses (Houssaye *et al.* 2021). In these species, the growth center is surrounded by highly anisotropic trabeculae, suggesting that this area is subjected to high stresses. Retaining a thick cortical layer around the growth center would then provide an additional adaptation to massive load support: instead of resorbing the bone, as is usual for non-graviportal species, the cortical bone around the growth center suggest a limited bone resorption resulting in a thick cortical layer capable of supporting massive loads. In both *D. giganteum* and *Mammuthus*, the compact bone is much thicker in the diaphysis, where it forms the cortical

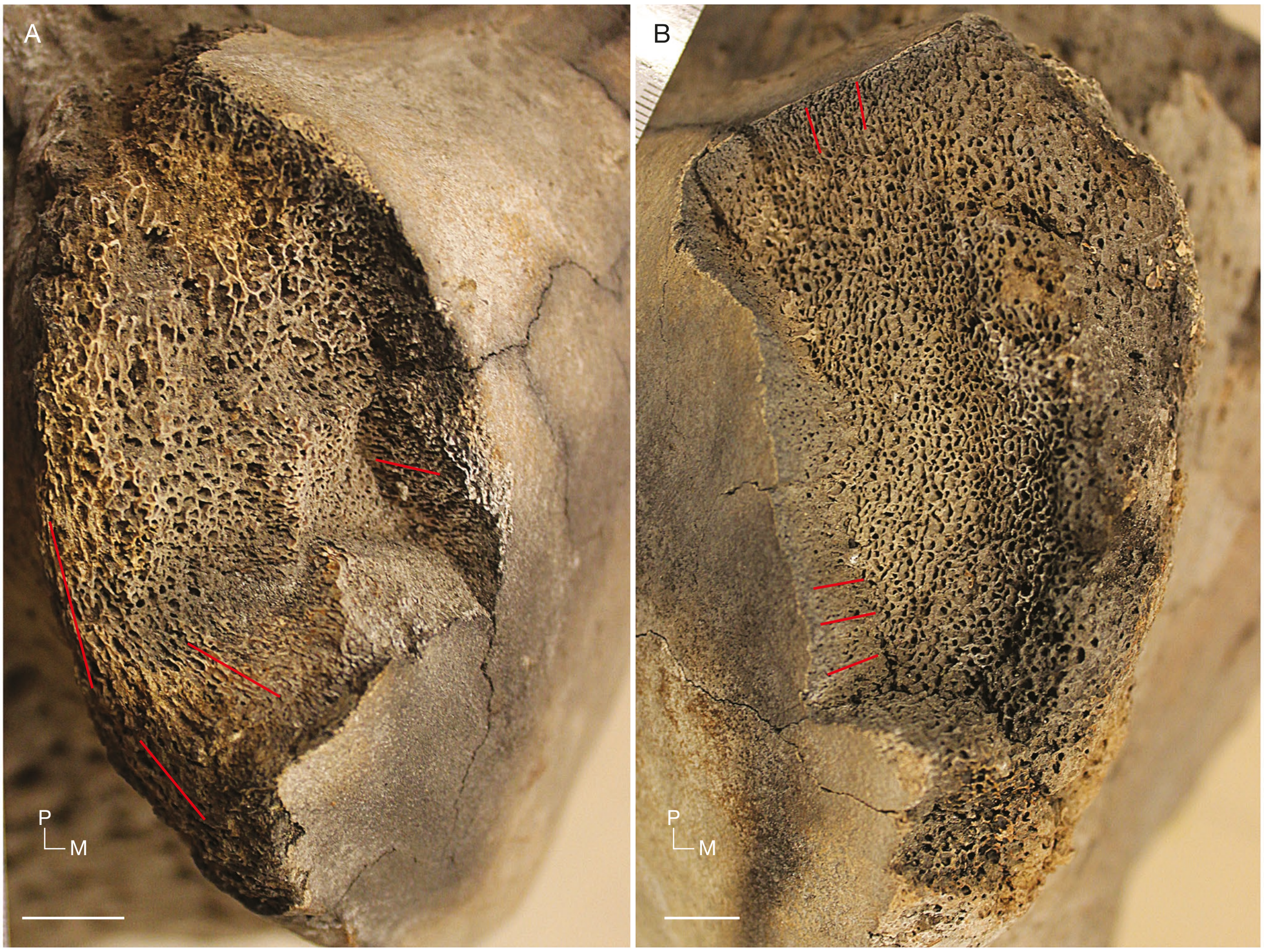

FIG. 5. — Zoomed-in views of trabecular orientation in the femur of HNHM-PAL 2025.5.1. of *Mammuthus* sp. in cranial view: **A**, lateral border; **B**, medial border. Abbreviations: **M**, medial; **P**, proximal. The **red lines** indicate the direction of the trabeculae in highly anisotropic areas. Photos by Camille Bader and Martin Segesdi. Scale bars: 1 cm.

bone, than in the epiphysis where it is limited to a thin layer. The trabecular tissue occupies a large portion of the diaphysis, leaving only the central part free, which corresponds to the growth center. This trabecular filling is typical of large quadrupeds (Houssaye *et al.* 2016), where an increased trabecular volume enhances load distribution along the bone, thereby improving weight-bearing capacity (Currey, 2002). This organizational pattern is consistently observed in other graviportal animals, including rhinoceroses, sauropod dinosaurs, and modern elephants (Etienne 2023; Lefebvre *et al.* 2023; Bader *et al.* 2025; Bader *et al.* in press).

Additionally, the trabeculae in the diaphysis are highly anisotropic, oriented parallel to the compact bone (i.e., proximodistally, orthogonally to the ground), which optimizes axial load distribution (Currey 2002, Barak *et al.* 2008). In modern elephants, this trabecular arrangement reflects the immense mechanical demands and the load application angle associated with a columnar stance, where the limb's long axis remains nearly perpendicular to the ground during standing and slow walking (Ren *et al.* 2010). Given the columnar posture of both *Deinotherium* and *Mammuthus*, the trabecular orientation in their femora similarly reflects limb orientation and weight-bearing adaptations. In the distal epiphysis, the trabeculae are less anisotropic than in the diaphysis, exhibiting a predominantly isotropic arrangement in the innermost part of the bone, and slightly increased anisotropy in the outermost part. This pattern reflects the diverse mechanical constraints to which the knee is subjected: the distal femoral epiphysis is part of the knee joint articulation, which imposes complex strain patterns beyond simple proximodistal loading. As a result, the trabeculae do not exhibit a strong preferential orientation. In the distal part of the trochlea, the trabeculae are orthogonal to the compact layer, facilitating optimal load distribution. Conversely, in the proximal part of the trochlea, which is not in direct contact with the tibia, the trabeculae are parallel to the compact layer, reflecting the different orientation of the mechanical strain.

INTERGENERIC VARIATION

While the femora of *D. giganteum* and *Mammuthus* sp. share an overall similar organization, we observed clear differences between the two species.

The hourglass-shaped distribution is clearly visible in *D. giganteum* but only slightly visible in *Mammuthus* sp. This variation may be linked to a number of factors: the two taxa might exhibit differences in posture and/or weight distribution. Conversely, if *D. giganteum* and *Mammuthus* sp. share a similar posture and weight distribution pattern along their craniocaudal axis, the observed difference might reflect different adaptive responses (e.g. relying more on thick cortex rather than on trabecular filling). In extant elephants, the hourglass-shaped distribution is more pronounced in the forelimb than in the hindlimb, the latter bearing approximately 40% of the body mass (Ren *et al.* 2010). The marked hourglass-shaped distribution in *D. giganteum* might then indicate a different weight distribution or adaptive strategy compared to that of extant elephants. Conversely, it is also possible that this pattern is more pronounced in the forelimb of *D. giganteum* as well: in this case, both *D. giganteum* and extant elephants would share the same overall pattern (hourglass-shaped distribution more pronounced in the forelimb) although in *D. giganteum*, this distribution would then be more accentuated across all limb bones. In *Mammuthus* sp., the less pronounced hourglass shape is unsurprising, as this species is more closely related to extant elephants. Additionally, mammoths generally have shorter hind limbs (Larramendi 2016), resulting in a greater weight load on the forelimbs and reduced strain on the hind limbs. *D. giganteum*, on the contrary, displays particularly high hips relative to their shoulder height (Larramendi 2016), thus increasing the relative weight on the hind limb, which might explain the more marked hourglass-shaped distribution in the femur, allowing for better resistance to mechanical loading.

The femoral cortex is relatively thinner in *Mammuthus* sp. (*RmaxT* = 0.11) than in *D. giganteum* (*RmaxT* = 0.36). This variation might be due to multiple factors: as with the cortical thickness distribution, differences in posture and limb proportions could result in a relatively lower mechanical load on the hindlimb of *Mammuthus*. Additionally, if the *Mammuthus* specimen studied here is indeed *Mammuthus primigenius* (*c.* 6000 kg; Larramendi 2016), it would be much lighter than *D. giganteum* (*c.* 12 000 kg; Larramendi 2016). As a result, *Mammuthus* would experience both lower absolute and relative weight constraints on its femur, leading to less pronounced weight-bearing adaptations. Conversely, this more slender build of the *Mammuthus* specimen might also suggest differences in overall weight distribution between the species, or different trade-offs between bone robustness (defined as the ratio of bone maximal length to the minimal diaphyseal circumference) and maximal cortical thickness. Indeed, in extant elephants *Elephas maximus* Linnaeus, 1758 display slightly more robust long bones than *Loxodonta africana* Cuvier, 1825 despite being lighter. However, *L. africana* shows slightly thicker cortices, which might compensate the lower robustness of the bones (Bader *et al.* 2025). In both *L. africana* and *E. maximus*, *RmaxT* falls between that of *D. giganteum* and *Mammuthus* sp., with values around 0.20-0.25 (measurements taken from Bader *et al.* 2025: fig. 6). This “intermediate” maximal relative thickness in extant elephants as compared to the two fossil taxa studied here highlights the range of possible trade-offs and adaptations to heavy weight-bearing in proboscideans. However, as only the femur is considered in this study, without the other long bones, our understanding of weight distribution and microanatomical adaptation in *D. giganteum* and *Mammuthus* sp. remains incomplete.

Another observed variation concerns the orientation of trabeculae in the center of the femoral shaft. In *Mammuthus*, the trabeculae around the growth center are oriented cranio-caudally, with a proximal inclination above the growth center and a distal inclination below it. This pattern is reminiscent of the trabecular arches observed around the growth center in extant elephant femora (Bader *et al.* 2025). Such an organization might function similarly to architectural arches, enhancing load distribution (Currey 2002). As such, we can hypothesize that pronounced arches might act as a compensating mechanism for a thinner cortex in *Mammuthus*, by distributing the load along the shaft. In *Deinotherium*, the presence of trabecular arches is not observable due to the incompleteness of the specimen and the presence of plaster fillings in the central part of the shaft. As a result, we cannot conclude on the possible link between the hourglass-shaped distribution of the cortex and the orientation of the trabeculae.

Microanatomical variations and morphotypes

The two femora analyzed in this study provide valuable new insights, particularly in the case of *D. giganteum*. While all proboscideans from the Miocene onwards exhibit columnar limbs, there is considerable variation in the external morphology of their bones (Bader *et al.* 2024) and in their limb proportions (Larramendi 2016; Belyaev *et al.* 2025). Graviportal proboscidean limb bones can be categorized into two main morphotypes: one characterized by relatively thin shafts and narrow epiphyses (including elephantids and deinotheres) and another with thicker shafts and larger epiphyses (including mammutids and gomphotheres) (Bader *et al.* 2024). Although these morphotypes are not absolute categories, they represent two biomechanical strategies for weight-bearing in graviportal proboscideans, and a such raise the question of potential associated microanatomical variations.

To our knowledge, all graviportal proboscidean specimens available for microanatomical analysis belong to either deinotheres or elephantids, i.e. from the same “thin” morphotype, so that no direct comparison has yet been made between the two morphotypes. Interestingly, the “thin” morphotype does not follow the phylogeny, as it evolved convergently in both elephantids and deinotheres (Bader *et al.* 2024). As such, this raises the question of whether this morphological similarity is associated with shared microanatomical adaptations. While limited by the scarce material, the present study provides partial insights: our findings suggest that in both *D. giganteum* and *Mammuthus*, trabecular bone adapts in a broadly similar manner to support massive body weight, reminiscent of what is observed in extant elephants. These results suggest that in both deinotheres and elephantids, the “thin” morphotype is associated with overall similar microanatomical features. However, we observed a clear difference in relative cortical thickness, which is much greater in the femur of *D. giganteum*. This variation may be linked to differences in absolute body mass, weight distribution or posture, but might also reflect distinct biomechanical strategies; further comparisons including complete bones of both species are needed to conclude on the link between external morphology and bone inner anatomy in relation to limb bone morphotype.

CONCLUSION

This study highlights key microanatomical adaptations in the femora of *Deinotherium* and *Mammuthus*, revealing a shared structural organization associated with graviportal weight-bearing. Both taxa exhibit thick cortical bone in the diaphysis, a medullary area largely filled with trabecular tissue, and highly anisotropic trabeculae aligned with axial loading. These patterns are similar to those observed in extant elephants, where they allow for efficient load distribution and mechanical resistance; our results thus highlight overall similar microanatomical adaptations to massive weight support among graviportal proboscidean taxa. Despite these global similarities, the femur of *D. giganteum* displays a more pronounced hourglass-shaped cortical distribution and greater relative cortical thickness than that of *Mammuthus*, suggesting potential differences in weight distribution and/or posture, or potentially different adaptive features of the bone microanatomy.

Acknowledgements

We warmly thank Erzsébet Latrán for providing the camera, and Mara Bader and János Magyar (HNHM, Budapest) for their assistance in moving heavy material. We would also like to thank Márton Szabó (HNHM, Budapest) for his help in the curatorial work. We are grateful to Ursula B. Göhlich (NHM, Vienna), Vlad Codrea (UBB, Cluj-Napoca), Ştefan Vasile (UniBuc, Bucharest), Márton Venczel (Muzeul Ţării Crişurilor, Oradea), and Attila Virág (ELTE, Budapest) for the useful consultations and for sharing literature. Many thanks to László Makádi (SARA, Budapest), Gábor Papp, Angéla Matuszka, Attila Vörös, János Szabó and Tibor Kecskeméti (HNHM, Budapest) for sharing their historical knowledge and helping us investigate the origin of bones. We are also grateful to two anonymous reviewers for their useful comments and suggestions, as well as Emmanuel Côtez (MNHN, Paris) and Sylvain Charbonnier (MNHN, Paris) for editorial work.

Credit statement

Conceptualization CB; Data curation CB, MG, MS; Formal Analysis CB; Investigation CB, MS; Methodology CB; Project Administration CB; Validation CB, MG, MS; Visualization CB; Writing – Original Draft Preparation CB; Writing – Review & Editing CB, MS.

Data availability

The 3D models are accessible on MorphoSource:

Deinotheriumsp001 (HNHM-V.79.166.) – https://doi.org/10.17602/M2/M630968;

HNHM-PAL 2025.5.1 – https://doi.org/10.17602/M2/M723153.

REFERENCES

Alexander R. M. N. & Pond C. M. 1992. — Locomotion and bone strength of the white rhinoceros, *Ceratotherium simum*. *Journal of Zoology* 227: 63-69. https://doi.org/10.1111/j.1469-7998.1992.tb04344.x

Andrews C. W. 1901. — Preliminary Note on some Recently Discovered Extinct Vertebrates from Egypt. (Part I.) *Geological Magazine* 8 (9): 400-409. https://doi.org/10.1017/S0016756800179282

Apostol L. 1968. — Particularité morphologiques des molaires de proboscidiens fossils quaternaires de Roumanie, conservées dans la collection du Musée d'Histoire Naturelle « Grigore Antipa ». *Travaux du Musée d'Histoire naturelle "Grigore Antipa"* 9: 581-616.

Bader C., Delapré A. & Houssaye A. 2023. — Shape variation in the limb long bones of modern elephants reveals adaptations to body mass and habitat. *Journal of Anatomy* 242 (5): 806-830. https://doi.org/10.1111/joa.13827

Bader C., Delapré A., Göhlich U. B. & Houssaye A. 2024. — Diversity of limb long bone morphology among proboscideans: how to be the biggest one in the family. *Papers in Palaeontology* 10 (6): e1597 https://doi.org.10.1002/spp2.1597

Bader C., Gilardet R., Herridge V., Hutchinson J. R. & Houssaye A. 2025. — Long bone microanatomy in elephants: microstructural insights into gigantic beasts. *Zoological Journal of the Linnean Society* 204 (3): zlaf008. https://doi.org/10.1093/zoolinnean/zlaf008

Bader C., Göhlich U. B. & Houssaye A. (in press). — Miniature giants: investigating limb long bone structure in dwarf Proboscideans. *Papers in Palaeontology*.

Barak M. M., Weiner S. & Shahar R. 2008. — Importance of the integrity of trabecular bone to the relationship between load and deformation of rat femora: an optical metrology study. *Journal of Materials Chemistry* 18 (32): 3855-3864. https://doi.org/10.1039/B805661G

Belyaev R. I., Boeskorov G. G., Kuznetsov A. N., Rotonda M. & Prilepskaya N. E. 2025. — Comparative study of the body proportions in Elephantidae and other large herbivorous mammals. *Journal of Anatomy* 246 (1): 63-85. https://doi.org/10.1111/joa.14143

Bertram J. E. A. & Biewener A. A. 1990. — Differential scaling of the long bones in the terrestrial carnivora and other mammals. *Journal of Morphology* 204 (2): 157-169. https://doi.org/10.1002/jmor.1052040205

Biewener A. A. 1989. — Scaling body support in mammals: limb posture and muscle mechanics. *Science* 245 (4913): 45-48. https://doi.org/10.1126/science.2740914

Biewener A. A. & Patek S. N. 2018. — *Animal Locomotion*. Oxford, United Kingdom, Oxford University Press, 240 p.

Bishop P. J., Hocknull S. A., Clemente C. J., Hutchinson J. R., Farke A. A., Barrett R. S. & Lloyd D. G. 2018. — Cancellous bone and theropod dinosaur locomotion. Part III—Inferring posture and locomotor biomechanics in extinct theropods, and its evolution on the line to birds. *PeerJ* 6: e5777. https://doi.org/10.7717/peerj.5777

Bonaparte C. L. 1845. — *Catalogo Metodico dei Mammiferi Europei*. Luigi di Giacomo Pirola, Valenciennes, Milan, 36 p. https://doi.org/10.5962/bhl.title.77311

Boros I. 1957. — The tragedy of the Hungarian Natural History Museum. Bibliotheca Kiadó, Budapest: 491-505.

Brookes J. 1828. — *A Catalogue of the Anatomical and Zoological Museum of Jeshua Brookes*. Esq., F.R.S. etc. Part 1. R.Taylor, London, 76 p.

Canoville A., Chinsamy A. & Angst D. 2022. — New comparative data on the long bone microstructure of large extant and extinct flightless birds. *Diversity* 14 (4): 298. https://doi.org/10.3390/d14040298

Cantalapiedra J. L., Sanisidro O., Zhang H., Alberdi M. T., Prado J. L., Blanco F. & Saarinen J. 2021. — The rise and fall of proboscidean ecological diversity. *Nature Ecology & Evolution* 5 (9): 1266-1272. https://doi.org/10.1038/s41559-021-01498-w

Carrano M. T. 1999. — What, if anything, is a cursor? Categories versus continua for determining locomotor habit in mammals and dinosaurs. *Journal of Zoology* 247: 29-42. https://doi.org/10.1111/j.1469-7998.1999.tb00190.x

Codrea V. A. 2008. — Fossil Proboscideans in inner Carpathian area (Romania). *Sargetia, Acta Musei Devensis* 21: 31-38.

Codrea V. A. & Andreica D. 1988. — Sur quelques restes de proboscidiens fossiles de Transylvanie. *Studia Universitatis Babeş-Bolyai, Geologie-Geografie., Cluj-Napoca* 33 (1): 89-96.

Codrea V. A., Răţoi B. G., Ursachi L. & Farcas C. 2002. — A large deinothere (Mammalia: Proboscidea) in the Late Miocene of the Moldavian Platform at Hhuşi (Vaslui County). *Muzeul Olteniei Craiova. Oltenia. Studii şi comunicări. Ştiinţele Naturii* 32 (1): 20-28.

Coombs W. P. 1978. — Theoretical aspects of cursorial adaptations in dinosaurs. *The Quarterly Review of Biology* 53 (4): 393-418. https://doi.org/10.1086/410790

Cubo J. 2004. — Pattern and process in constructional morphology. *Evolution and Development* 6 (3): 131-133. https://doi.org/10.1111/j.1525-142X.2004.04018.x

Currey J. D. & Alexander R. McN. 1985. — The thickness of the walls of tubular bones. *Journal of Zoology* 206 (4): 453-468. https://doi.org/10.1111/j.1469-7998.1985.tb03551.x

Currey J. D. 2002. — *Bones: Structure and Mechanics*. Princeton, NJ, Princeton University Press, 436 p.

Cuvier F. 1825. — Éléphant d'Afrique. *Histoire naturelle des Mammifères* 3: 1-2. https://doi.org/10.5962/bhl.title.78766

Doube M., Kłosowski M. M., Wiktorowicz-Conroy A. M., Hutchinson J. R. & Shefelbine S. J. 2011. — Trabecular bone scales allometrically in mammals and birds. *Proceedings of the Royal Society B: Biological Sciences* 278 (1721): 3067-3073. https://doi.org/10.1098/rspb.2011.0069

Éhik J. 1930. — *Prodinotherium hungaricum* n. g., n. sp. with an appendix by Szalay T. on the geological occurrence of *Prodinotherium hungaricum*. *Geologica Hungarica, ser. Palaeontologica* 6: 1-24

Eisenmann V. & Guérin C. 1984. — Morphologie fonctionnelle et environnement chez les périssodactyles. *Geobios* 17: 69-74. https://doi.org/10.1016/S0016-6995(84)80158-8

Etienne C. 2023. — *Biomechanical Adaptations to Support High Body Weight, an Investigation in Limb Long Bones of Rhinocerotoidea*. Unpublished Phd Thesis, Université Paris Cité, 405 p.

Falconer H. & Cautley P. T. 1846. — *Fauna antiqua sivalensis, being the Fossil Zoology of the Sewalik Hills, in the North of India*. Vol. 65. Smith, Elder and Company, London. https://doi.org/10.5962/bhl.title.61447

Gheerbrant E. 2009. — Paleocene emergence of elephant relatives and the rapid radiation of African ungulates. *Proceedings of the National Academy of Sciences of the United States of America* 106 (26): 10717-10721. https://doi.org/10.1073/pnas.0900251106

Gheerbrant E. & Tassy P. 2009. — L'origine et l'évolution des éléphants. *Comptes Rendus Palevol* 8 (2-3): 281-294. https://doi.org/10.1016/j.crpv.2008.08.003

Gheerbrant E., Sudre J. & Cappetta H. 1996. — A Palaeocene proboscidean from Morocco. *Nature* 383: 68-70. https://doi.org/10.1038/383068a0

Gheerbrant E., Sudre J., Tassy P., Amaghzaz M., Bouya B. & Iarochene M. 2005. — Nouvelles données sur *Phosphatherium escuilliei* (Mammalia, Proboscidea) de l'Éocène inférieur du Maroc, apports à la phylogénie des Proboscidea et des ongulés lophodontes. *Geodiversitas* 27 (2): 239-333. https://sciencepress.mnhn.fr/fr/periodiques/geodiversitas/27/2/nouvelles-donnees-sur-phosphatherium-escuilliei-mammalia-proboscidea-de-l-eocene-inferieur-du-maroc-apports-la-phylogenie-des-proboscidea-et-des-ongules-lophodontes

Gould S. J. 2002. — *The Structure of Evolutionary Theory*. Harvard University Press, 1464 p.

Gregory W. K. 1912. — Notes on the Principles of Quadrupedal Locomotion and on the Mechanism of the Limbs in Hoofed Animals. *Annals of the New York Academy of Sciences* 22 (1): 267-294. https://doi.org/10.1111/j.1749-6632.1912.tb55164.x

Habib M. B. & Ruff C. B. 2008. — The effects of locomotion on the structural characteristics of avian limb bones. *Zoological Journal of the Linnean Society* 153 (3): 601-624. https://doi.org/10.1111/j.1096-3642.2008.00402.x

Hajdú-Moharos J. 1997. — *Partium, A kapcsolt részek/A Királyhágómellék földrajzi leírása*. Királyhágómelléki Református Egyházkerület, Nagyvárad, 163 p.

Hays I. 1834. — Descriptions of the specimens of inferior maxillary bones of mastodons in the cabinet of the American Philosophical Society, with remarks on the genus *Tetracaulodon* (Godman). *Transactions of the American Philosophical Society* 4: 317-339. https://www.jstor.org/stable/1004835

Hildebrand M. 1974. — *Analysis of Vertebrate Structure*. New York, Wiley & Sons, 364 p.

Houssaye A., Waskow K., Hayashi S., Cornette R., Lee A. H. & Hutchinson J. R. 2016. — Biomechanical evolution of solid bones in large animals: a microanatomical investigation. *Biological Journal of the Linnean Society* 117 (2): 350-371. https://doi.org/10.1111/bij.12660

Houssaye A., Taverne M. & Cornette R. 2018. — 3D quantitative comparative analysis of long bone diaphysis variations in microanatomy and cross-sectional geometry. *Journal of Anatomy* 232 (5): 836-849. https://doi.org/10.1111/joa.12783

Houssaye A., Martin F., Boisserie J.-R. & Lihoreau F. 2021. — Paleoecological inferences from long bone microanatomical specializations in Hippopotamoidea (Mammalia, Artiodactyla). *Journal of Mammalian Evolution* 28 (3): 847-870. https://doi.org.10.1007/s10914-021-09536-x

Hutchinson J. R. & Pringle E. V. 2024. — Footfall patterns and stride parameters of common hippopotamus (*Hippopotamus amphibius*) on land. *PeerJ* 12: e17675. https://doi.org/10.7717/peerj.17675

Hutchinson J. R., Famini D., Lair R. & Kram R. 2003. — Are fast-moving elephants really running? *Nature* 422: 493-494. https://doi.org/10.1038/422493a

Illiger J. K. W. 1811. — *Prodromus Systematis Mammalium et Avium: Additis Terminis Zoographicis Utriusque Classis, Eorumque Versione Germanica*. Berolini: Sumptibus C. Salfeld, 62 p. https://doi.org/10.5962/bhl.title.106965

Jurcsák T. 1973. — Răspîndirea mastodonţilor la vest de Munţii Apuseni. *Nymphaea*. Muzeul Ţării Crişurilor, Oradea, 1: 313-341.

Jurcsák T. 1983. — Răspîndirea proboscidienilor în nord-vestul României. *Nymphaea*. Muzeul Ţării Crişurilor, Oradea, 10: 65-85.

Kaup J. 1829. — Neues Säugethiere, *Deinotherium*: *Deinotherium giganteum*. Isis, Iéna, 22 (4): 401-404.

Kingdon J. & Happold D. 2013. — *Mammals of Africa*. Vol. 1. Bloomsbury Publishing, 352 p.

Köhler M., Herridge V., Nacarino-Meneses C., Fortuny J., Moncunill-Solé B., Rosso A., Sanfilippo R., Palombo M. R. & Moyà-Solà S. 2021. — Palaeohistology reveals a slow pace of life for the dwarfed Sicilian Elephant. *Scientific Reports* 11 (1): 22862. https://doi.org/10.1038/s41598-021-02192-4

Koroknai I. 1954. — A Föld és az élet fejlődéstörténete (A Természettudományi Múzeum kiállítása). *Természet Társadalom Technika* 113 (6): 1-338.

Langman V. A., Roberts T. J., Black J., Maloiy G. M., Heglund N. C., Weber J. M., Kram R. & Taylor C. R. 1995. — Moving cheaply: energetics of walking in the African elephant. *Journal of Experimental Biology* 198: 629-632. https://doi.org/10.1242/jeb.198.3.629

Larramendi A. 2016. — Proboscideans: shoulder height, body mass and shape. *Acta Palaeontologica Polonica*. https://doi.org/10.4202/app.00136.2014

Lefebvre R., Allain R. & Houssaye A. 2023. — What's inside a sauropod limb? First three-dimensional investigation of the limb long bone microanatomy of a sauropod dinosaur, *Nigersaurus taqueti* (Neosauropoda, Rebbachisauridae), and implications for the weight-bearing function. *Palaeontology* 66 (4): e12670. https://doi.org/10.1111/pala.12670

Lefebvre R., Houssaye A., Mallison H., Cornette R. & Allain R. 2022. — A path to gigantism: three-dimensional study of the sauropodomorph limb long bone shape variation in the context of the emergence of the sauropod bauplan. *Journal of Anatomy* 241 (2): 297-336. https://doi.org/10.1111/joa.13646

Linnaeus C. 1758. — *Systema naturae per regna tria naturae, secundum classes, ordines, genera, species cum caracteribus, differentiis, synonymis, locis*. Editio decima, reformata, Vol I. Laurentii Salvii, Holmiae: 33. https://doi.org/10.5962/bhl.title.542

Magyar I., Botka D., Katona L., Harangi Sz., Lukács R. & Šujan M. 2025. — The Pannonian Stage: stratigraphy and geoenergy resources. *Geological Society, London, Special Publications* 554. https://doi.org/10.1144/SP554-2024-60

Mallet C., Cornette R., Billet G. & Houssaye A. 2019. — Interspecific variation in the limb long bones among modern rhinoceroses – extent and drivers. *PeerJ* 7: e7647. https://doi.org/10.7717/peerj.7647

Mallet C., Billet G., Houssaye A. & Cornette R. 2020. — A first glimpse at the influence of body mass in the morphological integration of the limb long bones: an investigation in modern rhinoceroses. *Journal of Anatomy* 237 (4): 704-726. https://doi.org/10.1111/joa.13232

Meshram S. N. & Sonakia A. 2006. — Fossil femur of a giant elephant (cf. *Elephas namadicus*) from Middle Pleistocene, central India. *Indian Minerals* 60: 199-202.

Nganvongpanit K., Siengdee P., Buddhachat K., Brown J. L., Klinhom S., Pitakarnnop T., Angkawanish T. & Thitaram C. 2017. — Anatomy, histology and elemental profile of long bones and ribs of the Asian elephant (*Elephas maximus*). *Anatomical Science International* 92 (4): 554-568. https://doi.org/10.1007/s12565-016-0361-y

Nikander R., Sievänen H., Heinonen A., Daly R. M., Uusi-Rasi K. & Kannus P. 2010. — Targeted exercise against osteoporosis: A systematic review and meta-analysis for optimising bone strength throughout life. *BMC Medicine* 8 (1): 47. https://doi.org/10.1186/1741-7015-8-47

Osborn H. F. 1929. — *The Titanotheres of Ancient Wyoming, Dakota, and Nebraska*. U.S. Geological Survey Monograph 55, 2 v. : col. front. (v.1) illus., plates. ; vol. 1: 1-701; vol. 2: 703-953. https://doi.org/10.3133/m55

Osborn H. F. 1936. — *Proboscidea. A Monograph of the Discovery, Evolution, Migration and Extinction of the Mastodonts and Elephants of the World*. Trustees of the American Museum of Natural History. https://doi.org/10.5962/bhl.title.12097.

Oxnard C. E. 1990. — From giant ground sloths to human osteoporosis: an essay on the architecture and biomechanics of bone. *Proceedings of the Australasian Society of Human Biology* 3: 75-96.

Oxnard C. E. 1993. — Bone and bones, architecture and stress, fossils and osteoporosis. *Journal of Biomechanics* 26: 63-79. https://doi.org/10.1016/0021-9290(93)90080-X

Papp G. 2016. — A Természettudományi Múzeum és 1956. A Nemzeti Múzeumban pusztító tűzvész előzményei, körülményei és következményei – The Hungarian Natural History Museum and the Hungarian Revolution of 1956. Fire in the building of the National Museum. *Annales Musei historico-naturalis hungarici* 108: 151-220.

Pohlig H. 1885. — Über eine Hipparionen-Fauna von Maragha in Nord-Persien, über fossile Elephantenreste Kaukasiens und Persiens und über die Resultate einer Monographie der fossilen Elephanten Deutschlands und Italien. *Zeitschrift der deutschen geologischen Gesellschaft, Berlin* 37 (4): 1022-1027.

Prothero D. R. & Sereno P. C. 1982. — Allometry and paleoecology of medial Miocene dwarf Rhinoceroses from the Texas Gulf Coastal Plain. *Paleobiology* 8: 16-30. https://doi.org/10.1017/S0094837300004322

Ren L., Miller C. E., Lair R. & Hutchinson J. R. 2010. — Integration of biomechanical compliance, leverage, and power in elephant limbs. *Proceedings of the National Academy of Sciences* 107 (15): 7078-7082. https://doi.org/10.1073/pnas.0911396107

Ross M. D. 1984. — The influence of gravity on structure and function of animals. *Advances in Space Research* 4: 305-314. https://doi.org/10.1016/0273-1177(84)90575-1

Ruff C. B. & Hayes W. C. 1983. — Cross-sectional geometry of Pecos Pueblo femora and tibiae—A biomechanical investigation: I. Method and general patterns of variation. *American Journal of Physical Anthropology* 60 (3): 359-381. https://doi.org/10.1002/ajpa.1330600308

Ruimerman R. 2005. — *Modeling and Remodeling in Bone Tissue*. PhD Thesis, Technische Universiteit Eindhoven. https://doi.org/10.6100/IR583545

Sanders W. J., Kappelman J. & Rasmussen D. T. 2004. — New large-bodied mammals from the late Oligocene site of Chilga, Ethiopia. *Acta Palaeontologica Polonica.* 49 (3): 365-392.

Schmidt-Nielsen K. 1984. — *Scaling: why is Animal Size so Important?* Cambridge University Press. https://doi.org/10.1017/CBO9781139167826

Shoshani J. & Tassy P. 2005. — Advances in proboscidean taxonomy and classification, anatomy and physiology, and ecology and behavior. *Quaternary International* 126: 5-20. https://doi.org/10.1016/j.quaint.2004.04.011

Stilson K. T., Hopkins S. S. & Davis E. B. 2016. — Osteopathology in Rhinocerotidae from 50 million years to the present. *PLoS One* 11 (2): e0146221. https://doi.org/10.1371/journal.pone.0146221

Sukumar R. 1992. — *The Asian Elephant: Ecology and Management*. Cambridge University Press, Cambridge, 256 p.

Szilágyi F. 2008. — *A Partium közigazgatási földrajza*. PhD dissertation. Debreceni Egyetem, Debrecen.

Tassy P. 1990. — The "Proboscidean Datum Event:" how many proboscideans and how many events?, *in* Lindsay E. H., Fahlbusch V. & Mein P. (eds), European Neogene Mammal Chronology. Springer: 237-252. https://doi.org/10.1007/978-1-4899-2513-8_16

Természettudományi Múzeum-Magyar Nemzeti Múzeum 1954. — *A Föld és az élet fejlődéstörténete kiállítás vezetője*. Boros, Budapest, 22 p.

Turner C. H. 1998. — Three rules for bone adaptation to mechanical stimuli. *Bone* 23 (5): 399-407. https://doi.org/10.1016/S8756-3282(98)00118-5

Wall W. P. 1983. — The correlation between high limb-bone density and aquatic habits in Recent mammals. *Journal of Paleontology* 57 (2): 197-207.

Wilson D. E., Mittermeier R. A. & Altrichter M. (eds) 2011. — *Handbook of the Mammals of the world.* 9 Volumes. Barcelona, Lynx Edicions.

Submitted on 14 April 2025;
accepted on 10 June 2025;
published on 16 April 2026.

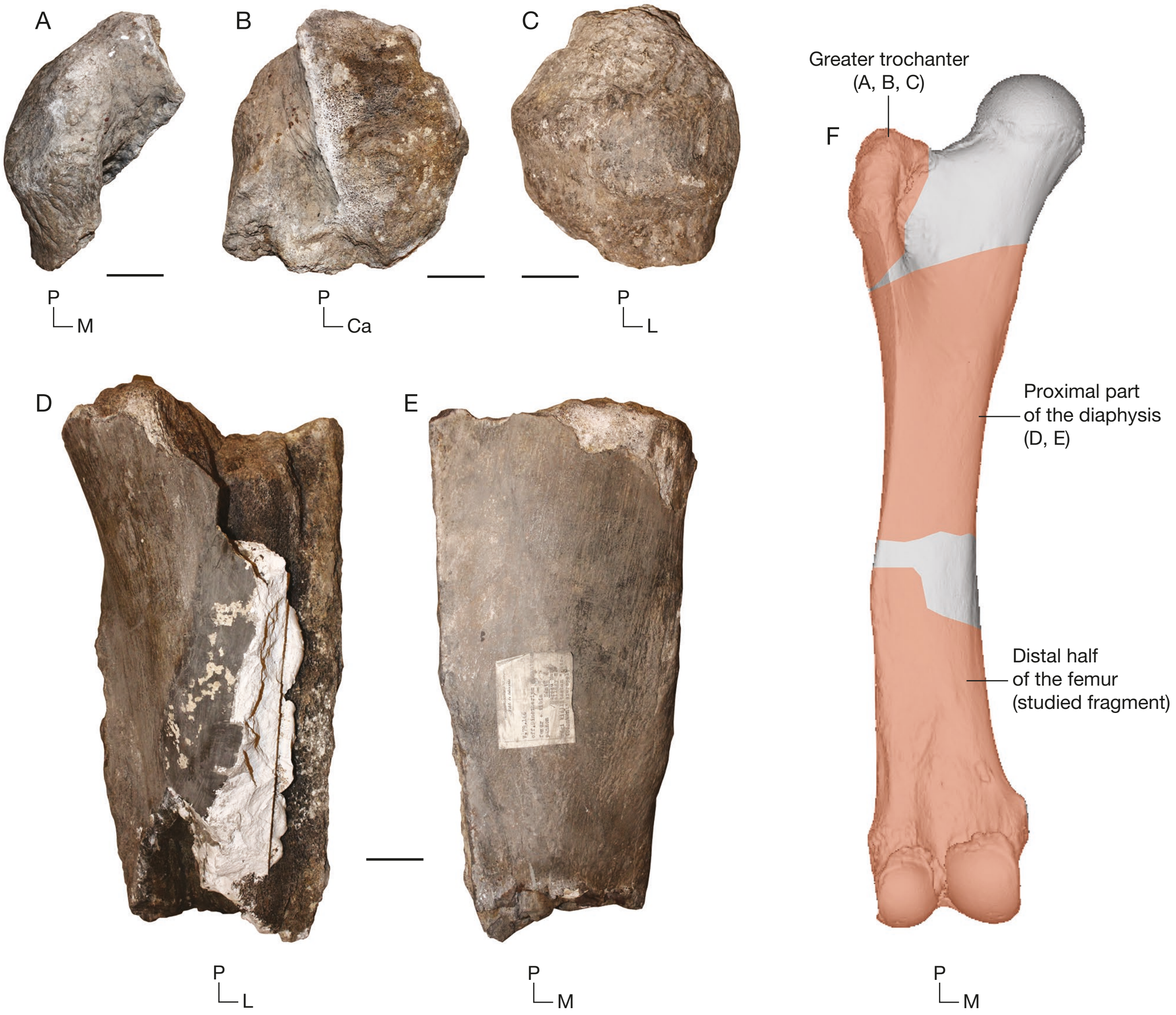

Fig. 6. — Supplementary Figure S1: remaining fragments of the HNHM-V.79.166. *Deinotherium giganteum* (Kaup, 1829) specimen (femur). **A**-**C**, greater trochanter; **D**, **E**, proximal half of the diaphysis; **F**, 3D model of a modern elephant with corresponding areas highlighted. Abbreviations: **Ca**, caudal; **L**, lateral; **M**, medial; **P**, proximal. Scale bars: 5 cm. photos by Camille Bader and Martin Segesdi, 3D model and illustration by Camille Bader.

FIG. 7. — Supplementary Figure S2: remaining fragments of the HNHM-V.79.166. *Deinotherium giganteum* (Kaup, 1829) specimen (tibia). **A**-**C**, proximal part of the diaphysis and proximal epiphysis; **D**, 3D model of a modern elephant tibia with the corresponding area highlighted. Abbreviations: **Cr**, cranial; **L**, lateral; **M**, medial; **P**, proximal. Scale bars: 5 cm. photos by Camille Bader and Martin Segesdi, 3D model and illustration by Camille Bader.

Fig. 8. — Supplementary Figure S3: The HNHM-V.79.166. *Deinotherium giganteum* (Kaup, 1829) specimen mounted in exhibition. The picture was provided by the Library of the Hungarian Natural History Museum.

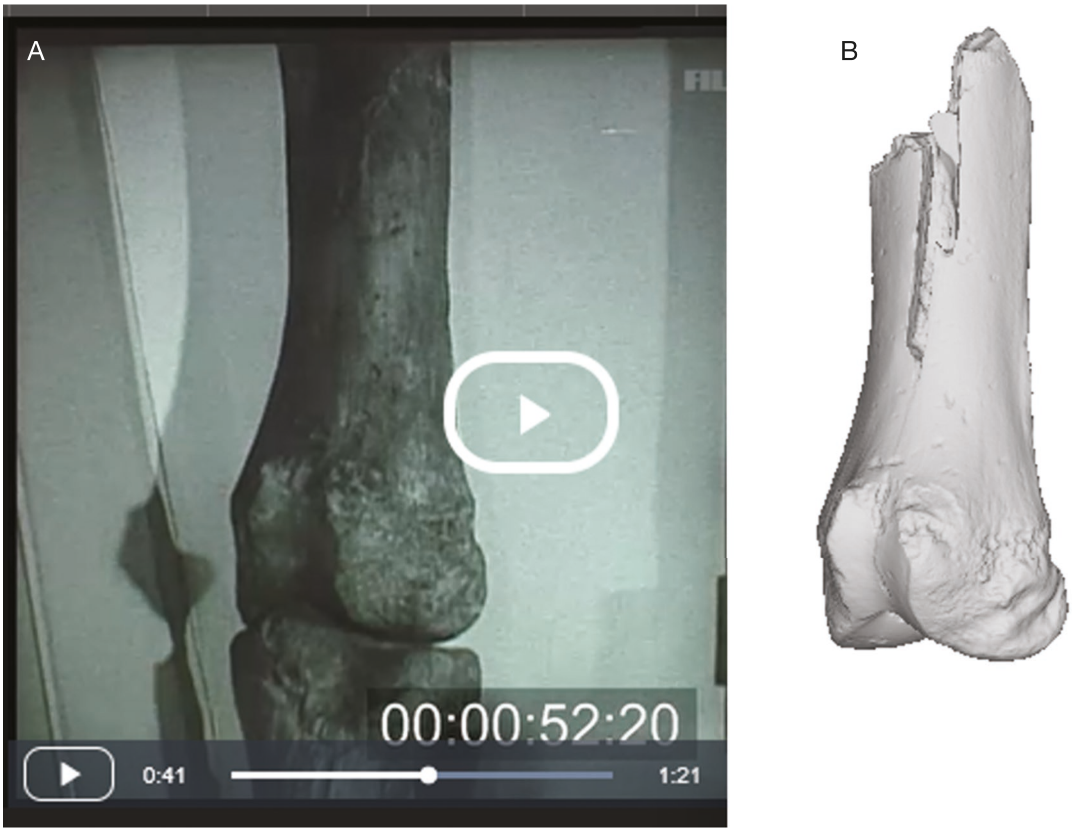

FIG. 9. — Supplementary Figure S4: comparison of the femur mounted in exhibition (**A**, newsreel clip from 1961.05.01) and the reconstructed 3D model of the broken specimen HNHM-V.79.166 (**B**). The video is accessible at https://filmhiradokonline.hu/watch.php?id=15855 [accessed March 18, 2025].